we do not have sufficient data to fully describe the equilibria that exist in solution, it would seem that these equilibria are more involved than the simple equilibrium proposed to exist between solvent-separated and contact ion pairs for analogous carbanions (e.g., $(C_6H_5)_3CNa$).[8,10,25]

The one-bond $^{31}P-^{13}C$ coupling constants for both phenylphosphine and diphenylphosphine (Table III) increase by a factor of 4 upon deprotonation of these hydrides. It is, however, quite possible that these couplings are negative since it has been suggested that a large separation in energy between valence s and p electrons may result in a negative one-bond coupling constant.[26] It is important to note that $^{31}P$ couplings frequently undergo a change of sign, and therefore a correlation with s character of the bonds is not possible until the signs are determined.

The two-bond couplings $J_{^{31}PC^{13}C}$ do not change magnitude upon deprotonation of either phenylphosphine or diphenylphosphine. Previous studies indicate that such couplings are always positive.[27] The three-bond couplings $J_{^{31}PCC^{13}C}$ also do not change upon deprotonation. All of the $^{31}P-^{13}C$ couplings, except the one-bond couplings in the anions, are of comparable magnitude to the analogous couplings in $(C_6H_5)_3P$.[28]

The one-bond $^{31}P-^{1}H$ couplings (Table III) are in reasonable agreement with the previously reported values. The significance of the reduction in the one-bond P-H coupling upon deprotonation of phenylphosphine is uncertain as the sign of the coupling was not determined. The three-bond couplings $J_{^{31}PCC^{1}H}$ of $C_6H_5PH_2$ and $(C_6H_5)_2PH$ are consistent with previously reported values.[29]

(25) Buncel, E.; Menon, B. *J. Chem. Soc., Chem. Commun.* **1978**, *758-759*.
(26) Weigert, F. J.; Roberts, J. D. *J. Am. Chem. Soc.* **1969**, *91*, 4940-4941.
(27) Mavel, G. *Annu. Rep. NMR Spectrosc.* **1973**, *5B* 71.
(28) Bodner, G. M.; Gaul, M. *J. Organomet. Chem.* **1975**, *101*, 63-69.
(29) Akitt, J. W.; Cragg, R. H.; Greenwood, N. N. *J. Chem. Soc., Chem. Commun.* **1966**, *134*-135.
(30) Stothers, J. B. "Carbon-13 NMR Spectroscopy"; Academic Press: New York, 1972; pp 199-200.

## Conclusions

Earlier conclusions that the $^{13}C$ para and $^{1}H$ para chemical shifts of neutral monosubstituted benzenes are linearly related to the $\pi$-electron density at the para carbon[6,7] can be extended to include anionic monosubstituted benzenes. The "corrected" $^{13}C$ para shift $(\delta_{^{13}C\ para} - \delta_{^{13}C\ meta})$[7] is a measure of the $\pi$-electron density at the para position caused by resonance with the anionic substituent. An analogous correction for the $^{1}H$ para chemical shift is probably much less reliable because the meta proton shifts appear to have relatively larger contributions from electric field and solvent effects than does that of the meta carbon.

The observed trends in the NMR chemical shifts indicate that there is a significant $p\pi-p\pi$ interaction between ring and substituent for the anions of the phenyl-substituted hydrides of phosphorus and arsenic which was not present in the neutral compounds. This resonance interaction in the anions is consistent with the increased acidity of these group 5B hydrides upon phenyl substitution.[3] We would predict that the anions of the phenyl-substituted hydrides of Si, Ge, and Sn would diplay comparatively small upfield shifts for the $^{13}C$ para resonances relative to the neutral hydrides and small values of $(\delta_{^{13}C\ para} - \delta_{^{13}C\ meta})$ in agreement with the reduced acidity of these hydrides upon phenyl substitution. Our observation that $C_6H_5PH_2$ is more acidic than $PH_3$ to approximately the same degree in both tetrahydrofuran and in liquid ammonia rules out the possibility that the use of different solvents could account for the observed relative acidity differences between the group 4B and group 5B compounds.

Ion-pairing equilibria are in effect in the solutions of the sodium salts as evidenced by the temperature- and concentration-dependent $^{31}P$ chemical shift of $C_6H_5PHNa$. These equilibria, however, have only a small effect on the $^{13}C$ chemical shifts.

**Registry No. 1**, 62-53-3; **2**, 638-21-1; **3**, 1073-41-2; **4**, 1865-45-8; **5**, 51918-31-1; **6**, 65423-92-9; **7**, 829-85-6; **8**, 122-39-4; **9**, 829-83-4; **10**, 5856-90-6; **11**, 4376-01-6; **12**, 41006-64-8; $PH_2Na$, 80243-05-6; $PH_3$, 7803-51-2.

# Comparative Studies of Mo-Mo and W-W Quadruple Bonds by SCF-X$\alpha$-SW Calculations and Photoelectron Spectroscopy

**F. Albert Cotton,*[1a] John L. Hubbard,[1b] Dennis L. Lichtenberger,[1b] and Irene Shim[1a]**

*Contribution from the Departments of Chemistry, Texas A&M University, College Station, Texas 77843, and University of Arizona, Tucson, Arizona 85721.* *Received April 29, 1981*

**Abstract:** The homologous compounds $M_2Cl_4(PR_3)_4$, with M = Mo and W, have been used in a combined theoretical and experimental study to compare the electronic structures of quadruple bonds between molybdenum atoms and between tungsten atoms. The theoretical work was carried out by the SCF-X$\alpha$-SW method on the model systems with R = H, but using in all other respects the experimentally measured bond lengths and angles for the compounds with R = $CH_3$. Relativistic corrections were made for both the molybdenum and tungsten compounds, but were found to be significant only for the tungsten compound. The $PMe_3$ compounds were used for measurements, made with both He I and He II excitation, of the photoelectron spectra in the gas phase. For both compounds the highest filled orbital is the M-M $\delta$-bonding orbital and the measured ionization energies are 6.44 and 5.81 eV for the Mo and W compounds, respectively. For both compounds the next observed ionizations, at 7.70 eV (Mo) and 7.05, 7.45 eV (W), can be assigned on experimental criteria to the M-M $\pi$-bonding orbitals. The spin-orbit splitting of the W-W $\pi$ peak shows features attributable to mixing of $\sigma$, $\pi$, and $\delta$ components by the spin-orbit coupling operator. These peaks are followed by ionizations assignable to M-P bonding electrons at 8.41 eV (Mo) and 8.36 eV (W). The calculations predict this order correctly for the W compound but reverse the Mo-Mo $\pi$ and Mo-P ionization energies. The W-W bonding appears to be weaker than the Mo-Mo bonding, and in general the results of this study are consistent with the greater reactivity (i.e., lower chemical stability) of the W-W quadruple bond as compared to the Mo-Mo quadruple bond.

The rapid and extensive development of the chemistry of the quadruply-bonded $Mo_2^{4+}$ unit over the past 16 years has not been matched by comparable fecundity in the chemistry of the $W_2^{4+}$ unit; advances in this chemistry have, instead, been fewer and hard won.[2] Gradually, however, a range of $W_2^{4+}$ compounds matching in composition, though usually not in ease of preparation or stability, those of $Mo_2^{4+}$ compounds is being elaborated. The

(1) (a) Texas A&M University. (b) The University of Arizona.
(2) Cotton, F. A.; Walton, R. A. "Multiple Bonds Between Metal Atoms"; John Wiley & Sons: New York, 1982.

0002-7863/82/1504-0679$01.25/0 

Table I. Splitting of Atomic Orbitals of $Mo_2Cl_4(PH_3)_4$ due to $D_{2d}$ Symmetry

| atom | orbitals | $D_{2d}$ symmetry |
|---|---|---|
| Mo | s | $a_1 + b_2$ |
| | $d_{z^2}$ | $a_1 + b_2$ |
| | $d_{x^2-y^2}$ | $a_1 + b_2$ |
| | $d_{xy}$ | $a_2 + b_1$ |
| | $d_{xz}, d_{yz}$ | 2e |
| Cl, P | s | $a_1 + b_2 + e$ |
| | $p_z$ | $a_1 + b_2 + e$ |
| | $p_x, p_y$ | $2e + a_1 + a_2 + b_1 + b_2$ |

difficulties encountered with the ditungsten compounds have persistently raised the question of how much intrinsic difference there might be between the Mo–Mo and W–W quadruple bonds, but compounds well suited to a comparative study have not been available.

What is required are relatively simple, compact molecules that are amenable to theoretical treatment, structural characterization, and spectroscopic (especially photoelectron spectroscopic) study. With the discovery by Sharp and Schrock[3] that $W_2Cl_4(PMe_3)_4$ can be fairly easily prepared and is a stable crystalline compound, it appeared that the time was auspicious for a comparative study since the molybdenum analogue was already a known compound[4] and its preparation can be accomplished efficiently.[5] The first step, namely, to determine accurately the structures of these two compounds, was soon accomplished[5] and their volatility and stability appeared to be such that gas-phase photoelectron spectra would be obtainable. The investigation described here was, therefore, undertaken.

## Procedures

**Calculations.** The SCF–Xα–SW method[6,7] was used. The model molecules used were $Mo_2Cl_4(PH_3)_4$ and $W_2Cl_4(PH_3)_4$. For both compounds we included relativistic corrections,[8] viz., Darwin, and mass-velocity for both core and valence metal orbitals.

The α values used were those of Schwarz[9] except for H, where a value of 0.77725 was chosen. The α value for W was extrapolated from Schwarz[10] as 0.69315. For inter- and outer-sphere regions a valence-electron weighted average of atomic α values was used.

The initial molecular potentials were superpositions of Herman–Skillman atomic potentials except for the metal atoms, where potentials derived from positively charged ions were employed. The atomic spheres were allowed to overlap, and their radii were chosen as 89% of the atomic number radii. The outer-sphere radius was chosen tangential to the outermost atomic sphere.

The SCF calculations for both molecules were converged nonrelativistically. Initially 5% of the new potential was mixed into the old potential. This percentage was gradually raised to 25% over ~70 iterations for the Mo compound and over ~60 iterations for the W compound. The calculations were considered to be converged when the shift in potential was less than 0.001 Ry, and in valence energy levels less than 0.0001 Ry. Thereafter, the relativistic corrections were added, and about 30 iterations were needed to reach convergence. On an Amdahl 470V/6 computer each iteration required about 50 s nonrelativistically and about 70 s relativistically. The ionization potentials for the highest levels of both molecules were calculated with Slater's transition-state method.[8]

The molecules were placed in a coordinate system with its origin at the midpoint of the M–M bond, the Z axis colinear with the M–M bond and the XZ and YZ planes each chosen to contain four ligand atoms.

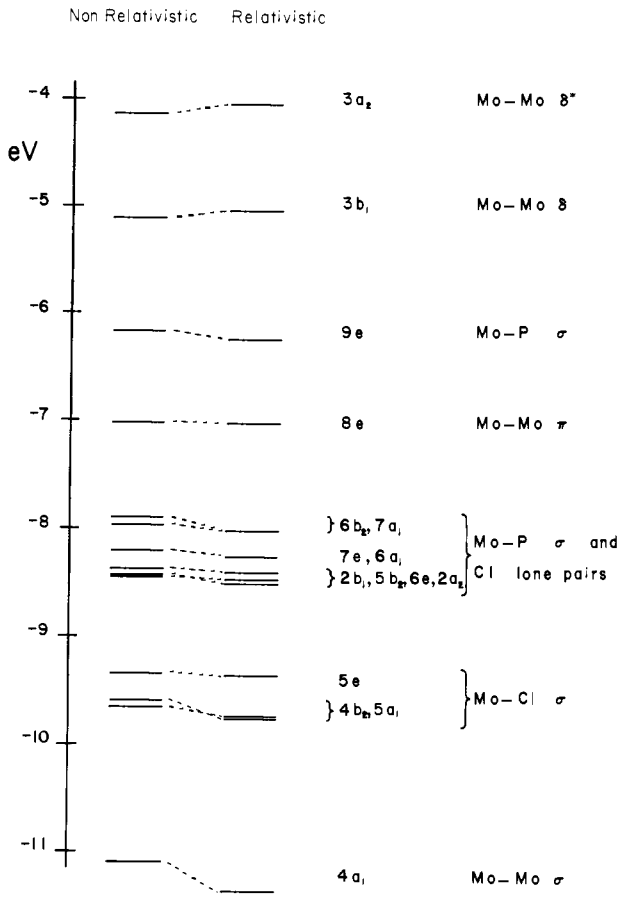


**Figure 1.** SCF–Xα–SW energy level diagram for $Mo_2Cl_4(PH_3)_4$. The diagram shows the occupied upper valence orbitals and the lowest lying unoccupied orbital (LUMO). It also illustrates the effects of relativistic corrections on the energy levels.

Each $PH_3$ ligand was oriented about the M–P bond so as to have the distal hydrogen atom in the XZ or YZ plane. The classification of atomic orbitals in the $D_{2d}$ symmetry is shown in Table I.

Bond distances and angles were taken from crystal structure data of the corresponding methyl compounds.[5] The geometry was, however, averaged according to $D_{2d}$ symmetry. Bond distances and angles for the Mo compound were Mo–Mo 2.130 Å, Mo–Cl 2.414 Å, Mo–P 2.545 Å, Mo–Mo–P 102.32°, and Mo–Mo–Cl 112.23°, and those for the W compound were W–W 2.262 Å, W–Cl 2.393 Å, W–P 2.507 Å, W–W–P 101.12°, and W–W–Cl 111.73°. For both compounds the P–H distance was chosen as 1.350 Å, and the metal–P–H angle as 109.47°.

The $D_{2d}$ symmetry-adapted linear combinations of atomic orbitals included s, p, d, and f spherical harmonics on Mo and W atoms, s, p, and d on P and Cl atoms, and s on H atoms. On the outer sphere, spherical harmonics up through $l = 6$ were included. The cores of the atoms were allowed to relax subject to the molecular environment at every iteration.

**Measurement of Photoelectron Spectra.** Spectra were obtained with an ESCA-36 photoelectron spectrometer. The variable temperature sample chamber and excitation sources were of our own design. He I radiation was from a differentially pumped capillary discharge lamp. He II radiation was from a differentially pumped charged particle oscillator lamp of the type described by Rabalais.[11]

He I spectra of both $Mo_2Cl_4[P(CH_3)_3]_4$ and $W_2Cl_4[P(CH_3)_3]_4$ were initially run at slowly increasing temperature on very small samples (~5 mg) to ensure that no transient features appeared from the time the sample began to sublime until sample depletion. Larger samples were then run at a particular temperature and again monitored from beginning to end for transient features. No unusual behavior was observed. The molybdenum spectra were obtained at 155 °C; the tungsten spectra were obtained at 165 °C. Slightly higher temperatures were used to enhance count rates for He II collections. He II collections were also repeated at least twice to establish reproducibility.

For comparison of the He I/He II ionization band cross sections, spectra have been corrected for the experimentally determined variation

(3) Sharp, P. R.; Schrock, R. R. *J. Am. Chem. Soc.* **1980**, *102*, 1430.
(4) Anderson, R. A.; Jones, R. A.; Wilkinson, G. *J. Chem. Soc., Dalton Trans.* **1978**, 446.
(5) Cotton, F. A.; Extine, M. W.; Felthouse, T. R.; Kolthammer, B. W. S.; Lay, D. G. *J. Am. Chem. Soc.* **1981**, *103*, 4040.
(6) Slater, J. C. "Quantum Theory of Molecules and Solids. The Self-Consistent Field of Molecules and Solids"; McGraw-Hill: New York, 1974; Vol. 4. Johnson, K. H. *Annu. Rev. Phys. Chem.* **1975**, *26*, 39. Johnson, K. H.; Norman, J. G., Jr.; Connolly, J. W. D. "Computational Methods for Large Molecules and Localized States in Solids"; Plenum Press: New York, 1972. Johnson, K. H. *Adv. Quantum Chem.* **1973**, *7*, 143.
(7) The program was written by Cook, M., Harvard University, and Bursten, B. E.; Stanley, G. G., Texas A&M University, 1979.
(8) Wood, J. H.; Bering, M. A. *Phys. Rev. B* **1978**, *18*, 2701.
(9) Schwarz, K. *Phys. Rev. B* **1972**, *5*, 2466.
(10) Schwarz, K. *Theor. Chim. Acta* **1974**, *34*, 225.
(11) Lancaster, G. M.; Taylor, J. A.; Ignatiev, A.; Rabalais, J. W. *J. Election Spectrosc. Relat. Phenom.* **1978**, *14*, 143.

Table II. Energies, Percent Contributions, and Percent Angular Contributions of the Highest Occupied Orbitals and the $\delta^*$ Orbital of $Mo_2Cl_4(PH_3)_4$

| | | | | | | % angular contribution | | | | | | | | | |
|---|---|---|---|---|---|---|---|---|---|---|---|---|---|---|---|
| | $-E$, eV | | % contribution | | | Mo | | | | Cl | | | P | | |
| level | nonrel | rel | Mo | Cl | P | s | p | d | f | s | p | d | s | p | d |
| $3a_2$ | 4.13 | 4.04 | 77 | 11 | 2 | 0 | 0 | 100 | 0 | 0 | 66 | 34 | | | |
| $3b_1$ | 5.11 | 5.04 | 72 | 14 | 1 | 0 | 0 | 100 | 0 | 0 | 80 | 20 | | | |
| 9e | 6.17 | 6.23 | 18 | 11 | 48 | 0 | 39 | 56 | 5 | 0 | 93 | 7 | 12 | 86 | 2 |
| 8e | 7.02 | 7.03 | 52 | 32 | 8 | 0 | 5 | 90 | 5 | 0 | 98 | 2 | | | |
| $7a_1$ | 7.89 | 8.01 | 23 | 40 | 23 | 30 | 9 | 57 | 4 | 0 | 100 | 0 | 6 | 89 | 5 |
| $6b_2$ | 7.96 | 8.02 | 18 | 41 | 25 | 15 | 0 | 83 | 2 | 0 | 100 | 0 | 10 | 84 | 6 |
| $6a_1$ | 8.19 | 8.25 | 16 | 43 | 24 | 12 | 4 | 84 | 0 | 0 | 100 | 0 | 8 | 86 | 6 |
| 7e | 8.20 | 8.25 | 3 | 84 | 1 | | | | | 0 | 100 | 0 | | | |
| $2a_2$ | 8.37 | 8.40 | 6 | 80 | 1 | | | | | 0 | 100 | 0 | | | |
| 6e | 8.37 | 8.42 | 5 | 74 | 6 | | | | | 0 | 100 | 0 | | | |
| $5b_2$ | 8.42 | 8.50 | 13 | 48 | 21 | 26 | 7 | 65 | 2 | 0 | 100 | 0 | 4 | 91 | 5 |
| $2b_1$ | 8.44 | 8.47 | 9 | 76 | 1 | | | | | 0 | 100 | 0 | | | |
| 5e | 9.33 | 9.36 | 38 | 59 | 1 | 0 | 3 | 94 | 3 | 0 | 98 | 2 | | | |
| $5a_1$ | 9.59 | 9.77 | 21 | 76 | 1 | 47 | 0 | 47 | 6 | 1 | 97 | 2 | | | |
| $4b_2$ | 9.65 | 9.73 | 25 | 73 | 1 | 12 | 2 | 84 | 2 | 1 | 97 | 2 | | | |
| $4a_1$ | 11.10 | 11.38 | 95 | 3 | 1 | 6 | 10 | 77 | 7 | | | | | | |

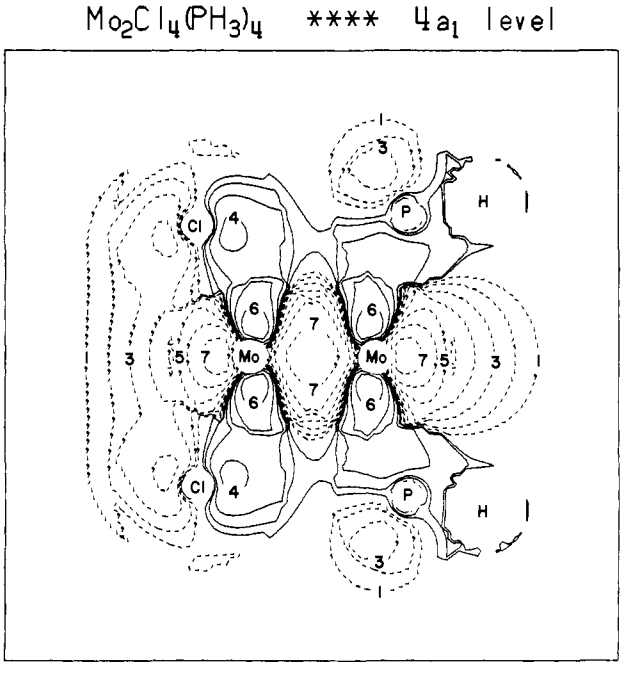


**Figure 2.** Contour plot of the $4a_1$ orbital of $Mo_2Cl_4(PH_3)_4$. Dashed lines indicate negative contour values. The lowest contour value (1) is 0.0050 e/au$^3$, and adjacent contours differ by a factor of 2. These contour values are used in all contour plots shown.

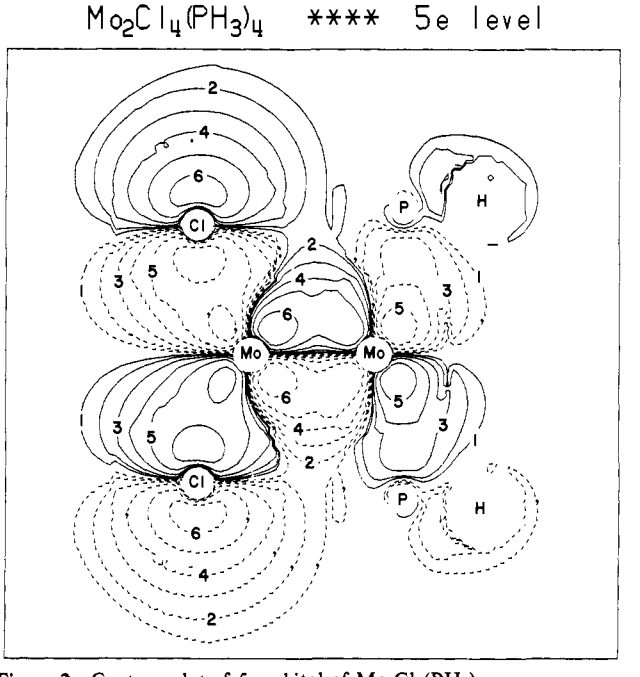


**Figure 3.** Contour plot of 5e orbital of $Mo_2Cl_4(PH_3)_4$.

of electron transmission with kinetic energy of the spectrometer analyzer. The He II $\alpha$ (40.81 eV) spectra have also been corrected for ionizations from the He II $\beta$ (48.4 eV, 12%) source excitation.

## Results and Discussion

**$Mo_2Cl_4(PR_3)_4$. Theory.** The theoretical results for the molybdenum model system, R = H, are presented in Figure 1 and Table II; only the LUMO and the orbitals principally involved in Mo–Mo and Mo–ligand bonding are given. Among the orbitals not shown are: (1) a group with energies of ca. −20 eV that are essentially pure chlorine 3s orbitals and play no significant role in bonding (as required by symmetry (cf. Table I) these are the $1a_1$, $1b_2$, and 1e orbitals.); (2) a group of orbitals originating from the phosphorus 3s atomic orbitals ($2a_1$, $2b_2$, 2e) which are located around −18.5 eV, and participate somewhat in the P–H bonding; and (3), in the energy range −13.42 to −13.26 eV, a group of six orbitals ($1b_1$, 3e, $1a_2$, $3a_1$, 4e, $3b_2$) which are essentially P–H bonding orbitals. Approximately half the charge in these orbitals is due to the P atoms, and the angular contributions from the P atoms consist of ~80% p character and ~20% d character. This significant amount of d character shows the importance of including spherical harmonics with $l = 2$ on P atoms in a calculation of this kind.

The energies of the remaining valence orbitals are listed in Table II and shown in Figure 1. These orbitals account for Mo–Mo, Mo–Cl, and Mo–P bonds, and also for Cl lone pairs. The relativistic corrections are clearly small. Even though this was the expected result, the calculation was carried out to obtain definitive proof that this is the case. For the quadruple bonds, where the d orbitals play such very different roles, relativistically induced differences would be expected to be greater than for most mononuclear complexes, so that is may also be safely inferred from the present results that relativistic corrections will, in general, cause only insignificant changes of the d-based orbitals of conventional compounds.

From Table II, which lists the relativistic as well as the nonrelativistic results, it is clear that many of the upper valence orbitals cannot be regarded as giving rise to localized bonds, since several of them have large contributions from Mo, Cl, and P atoms. However, some of them can. Thus, the lower lying orbital, $4a_1$, is almost entirely Mo–Mo $\sigma$ bonding, as seen in Figure 2, and the three orbitals between −9.7 and −9.3 eV can be characterized as

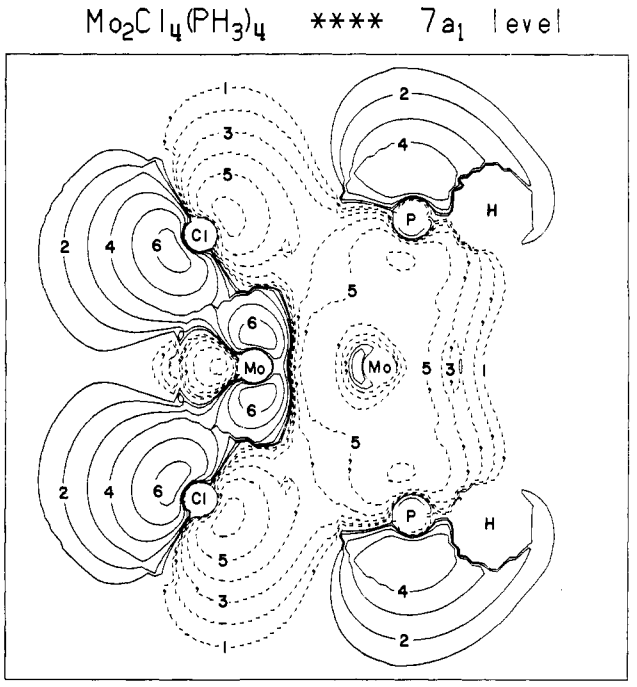


**Figure 4.** Contour plot of $7a_1$ orbital of $Mo_2Cl_4(PH_3)_4$.

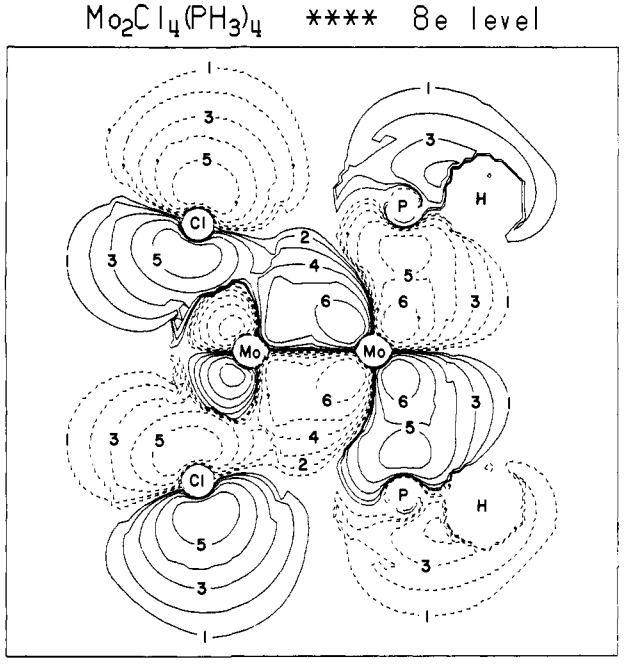


**Figure 5.** Contour plot of 8e orbital of $Mo_2Cl_4(PH_3)_4$.

Mo–Cl bonding orbitals, although the 5e orbital (Figure 3) also contributes to Mo–Mo $\pi$ bonding.

The next higher-lying set of orbitals, clustered between −8.5 and −7.8 eV, represents a mixture of Cl lone pairs and Mo–P bonds. As shown in Table II only four of the orbitals ($2b_1$, 6e, $2a_2$, 7e) can be characterized as Cl lone pairs. These represent all possible lone pairs perpendicular to the molecular axis (6e, $2a_2$, $2b_1$), but only two lone pairs parallel to the molecular axis (7e). The missing lone pairs, which should belong to the representations $a_1$ and $b_2$, are distributed among several orbitals $6a_1$, $7a_1$, $5b_2$, and $6b_2$, which are all of similar character. As may be seen in the contour plot of the $7a_1$ orbital in Figure 4, these orbitals also contribute considerably to the Mo–P $\sigma$ bonds.

The three highest lying occupied molecular orbitals are 8e, 9e, and $3b_1$. Two of these orbitals (8e and $3b_1$) are primarily Mo–Mo bonding. The 8e orbital (Figure 5) is mainly Mo–Mo $\pi$ bonding, although it also shows contributions from Cl lone pairs. The 9e

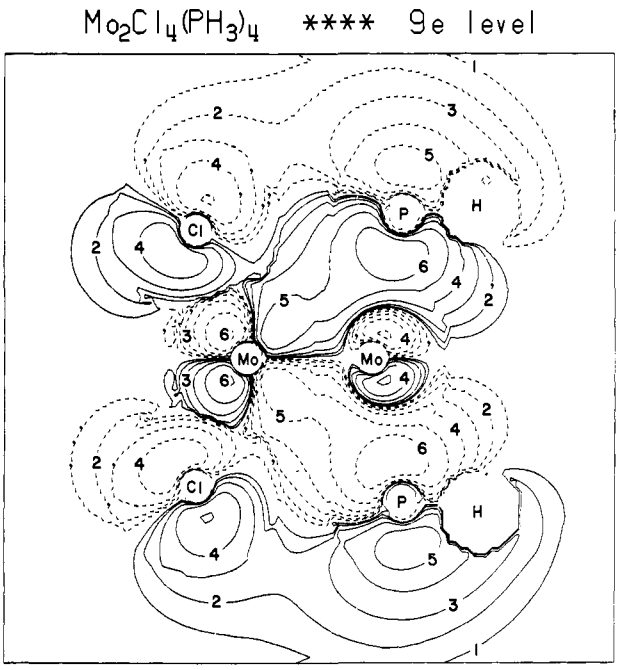


**Figure 6.** Contour plot of 9e orbital of $Mo_2Cl_4(PH_3)_4$.

orbital (Figure 6) serves mainly as a Mo–P $\sigma$-bonding orbital. The highest occupied molecular orbital (HOMO) is $3b_1$; this orbital has 72% Mo character, and it is predominantly a Mo–Mo $\delta$ orbital.

The lowest unoccupied molecular orbital (LUMO), $3a_2$, is essentially the $\delta^*$ orbital. The HOMO–LUMO gap, 0.98 eV, is typical of those found in other Mo–Mo quadruply-bonded systems. For example, in $[Mo_2Cl_8]^{4-}$ it is calculated to be 0.87 eV.[12] It is well known,[13] of course, that for several reasons, including orbital relaxation, but especially electron correlation, these orbital differences are far smaller than the observed energies of $\delta^2 \rightarrow \delta\delta^*$ transitions, and the present case is typical. The $^1A_1 \rightarrow {}^1B_2$ ($3a_2 \leftarrow 3b_1$) transition is observed[5] at $17.2 \times 10^3$ cm$^{-1}$ (2.13 eV).

It is evident that several features of the electronic structure are not amenable to simple descriptions. There is much mixing and delocalization, especially with respect to some of the chlorine lone pair orbitals and the Mo–P bonding orbitals. Indeed, these last deserve some special comment. It may seem strange that the energy of electrons in bonding orbitals (Mo–P $\sigma$) is as high as, or even a little higher than, the energy of some lone pair electrons (those on Cl atoms). This result at first caused us some concern, but it is, in fact, fully consistent with the structural information. As noted in papers reporting the structures of the $M_2Cl_4(PMe_3)_4$ and related compounds[5,14] the M–P bonds are anomalously long (by 0.10 to 0.15 Å) relative to the M–Cl bonds, when compared with the structure data for conventional $MX_2(PR_3)_2$ compounds, such as those of palladium(II) and platinum(II). This may be due to the fact that the d$\pi$ type orbitals and electrons of $Pd^{II}$ and $Pt^{II}$ that are available to strengthen and shorten the Pd–$PR_3$ and Pt–$PR_3$ bonds are relatively unavailable in the $M_2Cl_4(PR_3)_4$ molecules because they are utilized to form the $\pi$ and $\delta$ bonds between the metal atoms. Once it is recognized that the Mo–$PR_3$ and W–$PR_3$ bonds are unusually long, and therefore weak, and this is combined with the fact that the 3p orbitals of P lie several electron volts higher in energy than those of Cl because of the lower nuclear charge, it becomes understandable that the M–$PR_3$ $\sigma$ bonding electrons are not more tightly bound that the Cl lone pair electrons.

**$Mo_2Cl_4(PMe_3)_4$. PE Spectra.** We turn now to what we regard as the critical test of the correctness and accuracy of the calculation

(12) Norman, J. G.; Kolari, H. J. *J. Am. Chem. Soc.* **1975**, *97*, 33.
(13) Noodleman, L.; Norman, J. G., Jr. *J. Chem. Phys.* **1979**, *70*, 4903.
(14) Cotton, F. A.; Felthouse, T. R. *Inorg. Chem.* **1981**, *20*, 3880.

Table III. Calculated Ionization Potentials for $Mo_2Cl_4(PH_3)_4$ and $W_2Cl_4(PH_3)_4$

| $Mo_2Cl_4(PH_3)_4$ | | $W_2Cl_4(PH_3)_4$ | |
|---|---|---|---|
| level | IP,[a] eV | level | IP,[b] eV |
| $3b_1$ | 7.35 | $3b_1$ | 6.17 |
| 9e | 8.13 | 9e | 7.63 |
| 8e | 9.12 | 8e | (8.2) |
| $7a_1$ | 9.82 | $7a_1$ | (9.5) |

[a] From nonrelativistic transition-state calculations. [b] From relativistic transition-state calculations. [c] Values in parentheses were converged only to 0.1 eV.

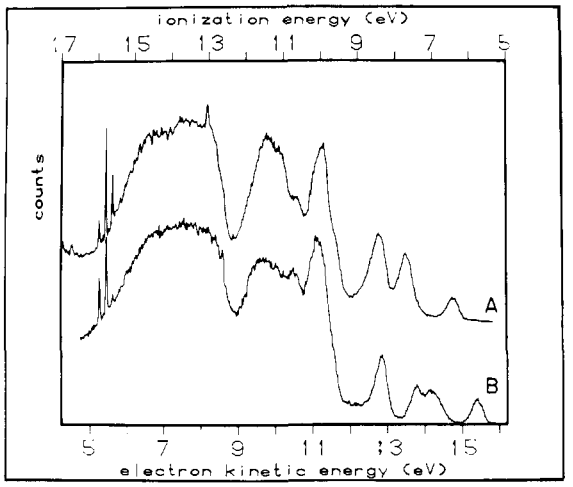


**Figure 7.** The He I photoelectron spectra of (A) $Mo_2Cl_4(PMe_3)_4$ and (B) $W_2Cl_4(PMe_3)_4$.

on $Mo_2Cl_4(PH_3)_4$, namely, the consistency between observed and calculated ionization energies.

In Table III we have listed some calculated ionization potentials for $Mo_2Cl_4(PH_3)_4$. The absolute values of the calculated ionization potentials are influenced by the choice of atomic and outer-sphere radii, and therefore only their relative values are of interest. It is also noteworthy that while the calculated values are for $Mo_2Cl_4(PH_3)_4$ the experimental results with which we shall be comparing them are for $Mo_2Cl_4(PMe_3)_4$. The greater inductive effect of the methyl groups will cause the observed values to be lower than those calculated. According to the calculations the separation between the first two peaks should be about 0.8 eV, and that between the second and third about 1.0 eV. At about 0.7 eV higher energy a strong band should appear, followed closely by many other overlapping ones.

The He I photoelectron spectrum of $MoCl_4(PMe_3)_4$ between 5 and 17 eV is shown in Figure 7 and the He I and He II spectra of the low-energy ionizations are compared in Figure 8. The data are tabulated in Table IV. In terms of number and approximate positions of bands the agreement with theory is excellent. However, if we make the usual assumption that the ionization cross sections on going from He I to He II will increase more for metal-based orbitals than for ligand-based ones, we are forced to conclude that the second observed band has considerably more metal character than the third, contrary to the theoretical results. Both of the levels are of e symmetry and they are similar in energy; the question is one of how the Mo–Mo $\pi$ and Mo–P $\sigma$ characters are distributed between the two. The calculation appears to have reversed the attributions of predominance, but it is not clear why. It does not seem likely that using $PH_3$ ligands instead of $PMe_3$ ligands could be reasonable for this, and, as will be seen, the correct ordering of the ionizations is obtained for the tungsten compound.

**$W_2Cl_4(PR_3)_4$. Theory.** The results of the calculations are displayed in Figure 9, which shows both the nonrelativistic levels and those obtained after the approximate relativistic corrections have been applied. The energies of the relativistic MO's and the atomic contributions to them are presented in Table V. The MO's arising from chlorine and phosphorus 3s orbitals and those which

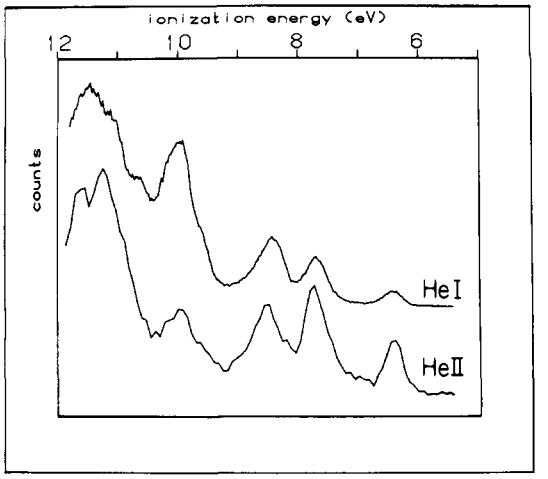


**Figure 8.** The He I and He II photoelectron spectra of $Mo_2Cl_4(PMe_3)_4$.

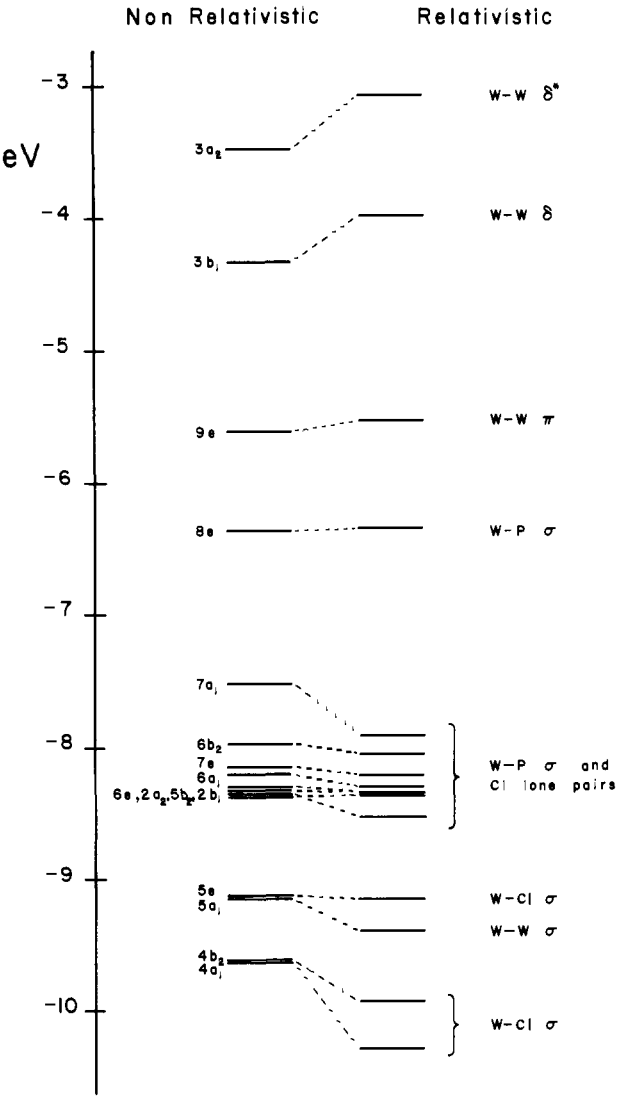


**Figure 9.** SCF–X$\alpha$–SW energy level diagram for $W_2Cl_4(PH_3)_4$. The occupied upper valence orbitals are shown as well as the lowest lying unoccupied orbital (LUMO). The diagram also shows the changes in the energy levels due to relativistic corrections.

are essentially P–H bonding orbitals are very similar to the corresponding ones in the molybdenum compound (vide supra) and are omitted from Figure 9 and Table V.

At first glance Figure 9 shows a great similarity to Figure 1. In each case the three highest-lying occupied molecular orbitals

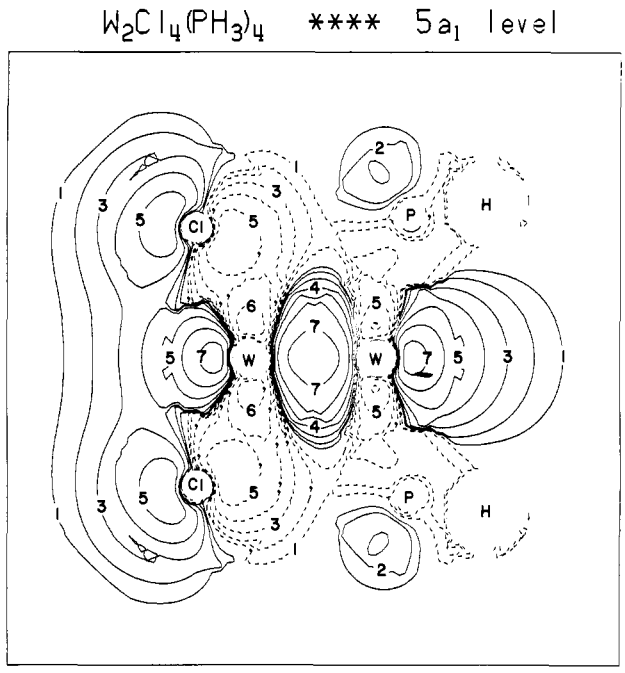


**Figure 10.** Contour plot of $5a_1$ orbital of $W_2Cl_4(PH_3)_4$.

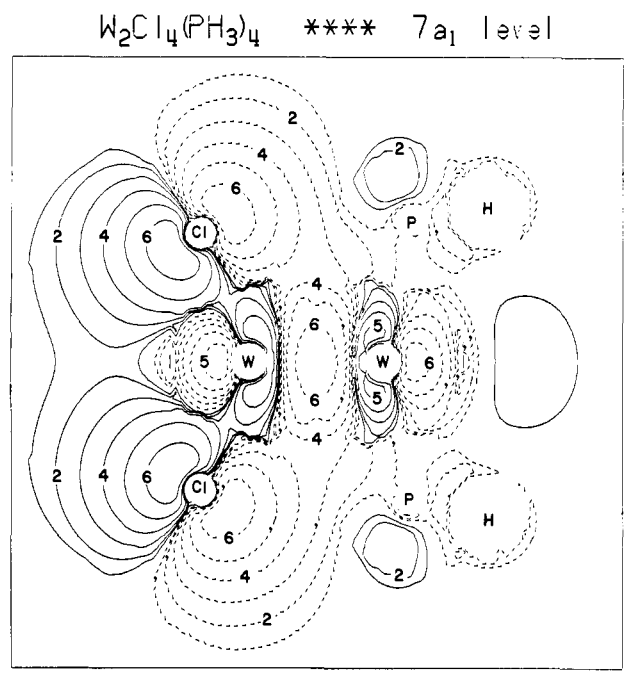


**Figure 11.** Contour plot of $7a_1$ orbital of $W_2Cl_4(PH_3)_4$.

Table IV. Peak Positions and Relative Peak Area for Low-Energy Bands[a]

| position, eV | half-width, eV | area | |
|---|---|---|---|
| | | He I | He II |
| | $Mo_2Cl_4(P(CH_3)_3)_4$ | | |
| 6.44 | 0.35 | 1.0 | 1.0 |
| 7.70 | 0.41 | 3.2 | 2.2 |
| 8.41 | 0.49 | 5.5 | 2.2 |
| 9.98 | 0.76 | ~20 | ~2 |
| | $W_2Cl_4(P(CH_3)_3)_4$ | | |
| 5.81 | 0.32 | 1.0 | 1.0 |
| 7.05 | 0.58 | 3.9 | 2.5 |
| 7.45 | 0.30 | | |
| 8.36 | 0.34 | 3.2 | 0.63 |
| 10.06 | 0.58 | ~30 | ~4 |

[a] Peak positions and relative areas from program GFIT described in: Lichtenberger, D. L.; Fenske, R. F. *J. Am. Chem. Soc.* 1976, *98*, 50.

are well separated from each other, and also from eight closely spaced lower-lying levels. Moreover, the four lowest-lying MO's are again concerned with M–M and M–Cl bonding. There are, however, several important differences. The orbital mainly responsible for W–W $\sigma$ bonding, $5a_1$, is located among, rather than below, the W–Cl $\sigma$-bonding orbitals. This may, though it need not necessarily, imply a weaker metal–metal bond in the tungsten compound; the contour plot of this orbital, shown in Figure 10, is quite similar to the main Mo–Mo $\sigma$-bonding orbital ($4a_1$) which is shown in Figure 2. The $4a_1$ orbital which is primarily a W–Cl $\sigma$-bonding orbital has a small admixture of W–W $\sigma$. This is partly due to the relativistic corrections causing a change of W contribution from 28% to 37%. The relativistic corrections also cause the W angular contributions in this orbital to change from 12% s and 81% d to 73% s and 19% d.

The closely spaced levels between −7.90 and −8.52 eV account for W–P $\sigma$ bonding and Cl lone pairs. Just as for $Mo_2Cl_4(PH_3)_4$ the Cl lone pairs perpendicular to the molecular axis can be clearly identified with the orbitals $2b_1$, $2a_2$, and 6e. For the Mo compound only a single orbital (7e) could be associated with the Cl lone pairs parallel to the molecular axis. In the case of the W compound both 7e and $7a_1$ are Cl lone-pair orbitals parallel to the molecular axis, although the $7a_1$ orbital also has an admixture of W–W $\sigma$-bonding characteristics, as may be seen in Figure 11. In

Table V. Energies, Percent Contributions, and Percent Angular Contributions of the Highest Occupied Orbitals and the $\delta^*$ Orbital of $W_2Cl_4(PH_3)_4$ Resulting from Xα–SW Calculations Including Relativistic Corrections

| | | | | | | % character | | | | | | | | | |
|---|---|---|---|---|---|---|---|---|---|---|---|---|---|---|---|
| | −E, eV | | % contribution | | | W | | | | Cl | | | P | | |
| level | nonrel | rel | W | Cl | P | s | p | d | f | s | p | d | s | p | d |
| $3a_2$ | 3.46 | 3.05 | 71 | 12 | 4 | 0 | 0 | 100 | 0 | 0 | 55 | 45 | | | |
| $3b_1$ | 4.32 | 3.96 | 68 | 13 | 3 | 0 | 0 | 100 | 0 | 0 | 67 | 33 | | | |
| 9e | 5.60 | 5.52 | 64 | 11 | 9 | 0 | 10 | 88 | 2 | 0 | 86 | 14 | | | |
| 8e | 6.35 | 6.35 | 19 | 14 | 48 | 0 | 24 | 68 | 8 | 0 | 96 | 4 | 12 | 85 | 3 |
| $7a_1$ | 7.51 | 7.90 | 22 | 71 | 1 | 15 | 26 | 55 | 4 | 0 | 100 | 0 | | | |
| $6b_2$ | 7.96 | 8.03 | 13 | 56 | 16 | 14 | 1 | 83 | 2 | 0 | 100 | 0 | 11 | 82 | 7 |
| 7e | 8.13 | 8.19 | 3 | 83 | 0 | | | | | 0 | 100 | 0 | | | |
| $6a_1$ | 8.18 | 8.28 | 33 | 8 | 43 | 12 | 0 | 86 | 2 | | | | 7 | 87 | 6 |
| $2a_2$ | 8.32 | 8.33 | 5 | 80 | 1 | | | | | 0 | 100 | 0 | | | |
| 6e | 8.27 | 8.33 | 4 | 74 | 7 | | | | | 0 | 100 | 0 | | | |
| $2b_1$ | 8.36 | 8.35 | 7 | 78 | 2 | | | | | 0 | 100 | 0 | | | |
| $5b_2$ | 8.34 | 8.52 | 22 | 28 | 31 | 21 | 4 | 75 | 0 | 0 | 99 | 1 | 4 | 90 | 6 |
| 5e | 9.11 | 9.13 | 22 | 75 | 0 | 0 | 16 | 81 | 3 | 0 | 99 | 1 | | | |
| $5a_1$ | 9.14 | 9.38 | 79 | 20 | 1 | 7 | 9 | 80 | 4 | 0 | 97 | 3 | | | |
| $4b_2$ | 9.71 | 9.92 | 22 | 77 | 1 | 36 | 4 | 57 | 3 | 2 | 96 | 2 | | | |
| $4a_1$ | 9.74 | 10.27 | 37 | 58 | 4 | 73 | 2 | 19 | 6 | 3 | 95 | 2 | | | |

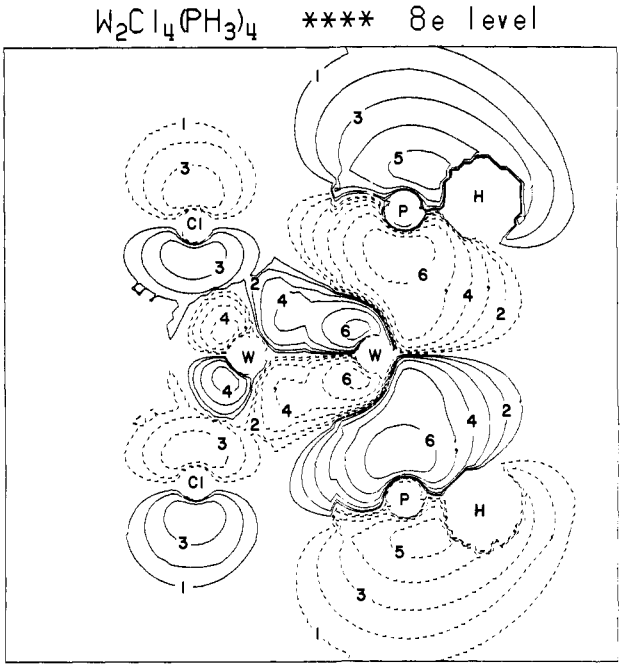


**Figure 12.** Contour plot of 8e orbital of $W_2Cl_4(PH_3)_4$.

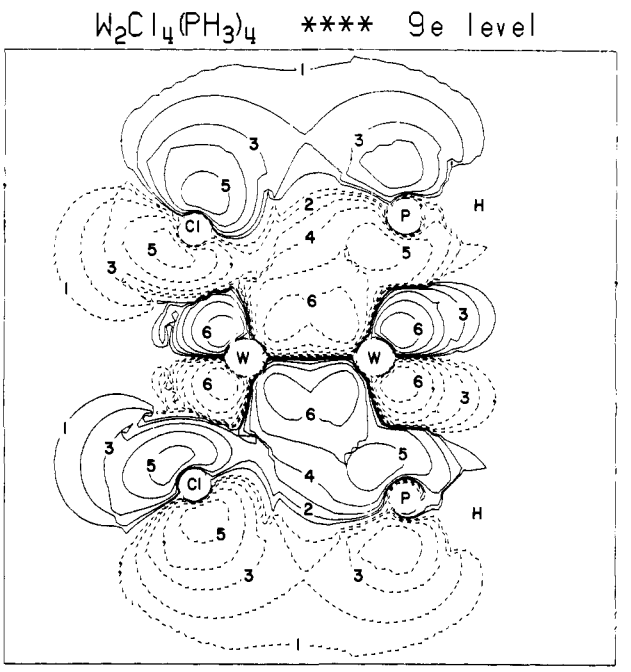


**Figure 13.** Contour plot of 9e orbital of $W_2Cl_4(PH_3)_4$.

contrast to the $6a_1$ orbital of $Mo_2Cl_4(PH_3)_4$, the $6a_1$ orbital of $W_2Cl_4(PH_3)_4$ does not contain Cl lone pairs, but is distinctly a W–P $\sigma$-bonding orbital. The missing Cl lone pair is distributed among the orbitals $5b_2$ and $6b_2$, although the $5b_2$ orbital is mainly a W–P $\sigma$-bonding orbital.

The separation of Cl lone pairs and W–P $\sigma$ bonds among different orbitals is seen only after the relativistic corrections. The Cl contributions in the $6a_1$ and $7a_1$ nonrelativistic orbitals are 25% and 41%, respectively, but these change to 8% and 71% after application of the relativistic corrections. Likewise, the nonrelativistic Cl contributions to $5b_2$ and $6b_2$ are 42% and 44%, but change to 28% and 56% relativistically. Thus, the relativistic corrections cause the lower-lying orbitals ($5b_2$, $6a_1$) to lose Cl contributions while the higher lying orbitals ($6b_2$, $7a_1$) gain Cl contributions. Altogether, this probably stabilizes the molecule, since the bonding orbitals are lowered energetically, while the nonbonding orbitals are raised.

The effect of the relativistic corrections on the $3b_1$ ($\delta$ bonding) level is to raise it in energy. This, and all the other effects of applying the relativistic corrections mentioned above, is similar to what was observed in applying relativistic corrections to the $[Re_2Cl_8]^{2-}$ ion.[15]

The nature of the 8e and 9e orbitals in $W_2Cl_4(PH_3)_4$ is of particular interest. In contrast to the result for the molybdenum analogue, we find here that the 8e orbital (Figure 12) has predominantly W–P $\sigma$-bonding character and the 9e orbital (Figure 13) is predominantly W–W $\pi$ bonding. The relatively clear differentiation between the two orbitals arises when the relativistic corrections are made, since the tungsten contribution to 9e is changed from 48% to 64%.

**$W_2Cl_4(PMe_3)_4$. PE Spectra.** As shown in Table III the photoelectron spectrum is expected to show $3b_1$, 9e, and 8e ionizations as its first three features with the first two being from metal-dominated MO's. The observed He I and He II spectra, shown in Figure 14, agree very well with this prediction. The second peak is split by spin–orbit coupling, which is qualitatively to be expected even though our method of calculation does not explicitly produce it. We shall return to this later. The enhancement of the ionization cross section for the first two peaks compared to the third on going from He I to He II is in good agreement with the characters of the $3b_1$, 9e, and 8e orbitals, namely, as W–W $\delta$, W–W $\pi$, and W–P $\sigma$, respectively.

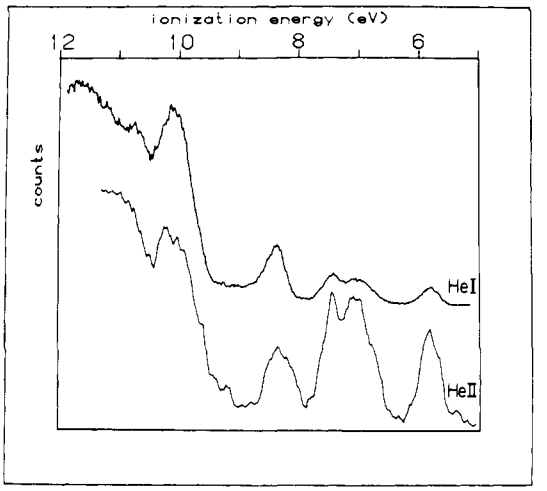


**Figure 14.** The He I and He II photoelectron spectra of $W_2Cl_4(PMe_3)_4$.

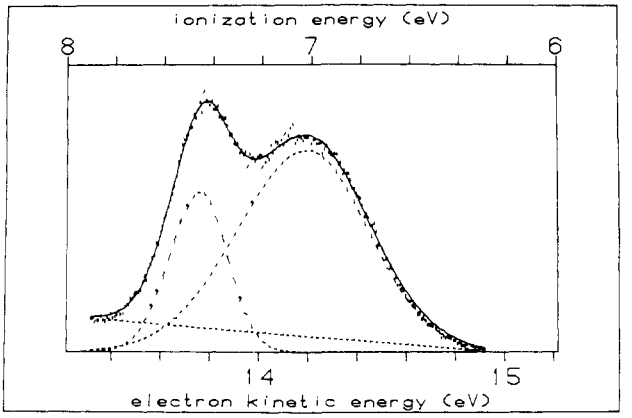


**Figure 15.** A least-squares curve fit of the contour of the $\pi$ ionization in the He I spectrum of $W_2Cl_4(PMe_3)_4$ into the asymmetric Gaussian components resulting from spin–orbit coupling. The points are the data, the dashes are the base line and curve fit bands, and the solid line is the fit sum.

Quantitatively, there are only minor discrepancies between the predicted and observed peak positions; the separation of the first

(15) Unpublished work by B. E. Bursten, F. A. Cotton, P. E. Fanwick and G. G. Stanley. The energy level diagram showing the results has been published. See: Cotton, F. A. *J. Mol. Struct.* **1980**, *59*, 97.

peak and the midpoint of the second doublet are predicted within about 0.1 eV, but the observed separation of the 9e and 8e ionizations is about 0.5 eV greater than that calculated. This should be considered as fairly good agreement for such a complex molecule.

A careful examination of the second, split peak in the PE spectrum, which we assign to ionization of the W-W $\pi$ electrons, leaves little doubt that the two spin-orbit components have different band envelopes and cross sections, as shown in Figure 15. This is not anomalous since the two components of the split $\pi$ level are rendered inequivalent by their different couplings to the $\sigma$ and $\delta$ levels. The $\pi$ level with $j = {}^3/_2$ is coupled to the $\delta$ level while the $\pi$ level with $j = {}^1/_2$ is coupled to the $\sigma$ level.

Figure 7 shows that the only substantial differences between the ionizations of the Mo and W complexes involve the predominantly metal levels. These particular differences are large in comparison to the normal changes found between the ionizations of mononuclear complexes from the first, second, and third transition-metal series. The first ionization of the W complex occurs at 0.63 eV lower binding energy than the first ionization of the Mo complex, and hence the W complex is much more easily oxidized. The predominantly metal $\pi$ ionization of the W complex occurs at 0.25-0.65 eV lower binding energy than the corresponding ionization of the Mo complex. In contrast to these substantial changes in the metal ionizations, the changes in the M-P $\sigma$, M-Cl $\sigma$, and Cl lone pair ionizations are quite small (less than 0.1 eV). This indicates that the destabilization of the predominantly metal levels of the W complex is not a simple result of the inherent atomic orbital energy or "electronegativity" for the W atom, since this would also result in a greater negative charge on the ligands and a shift of their ionizations.

Apparently the instability of the W systems resides with the metal atoms and the metal-metal interactions, and not with metal-ligand or ligand-ligand interactions. It seems likely that the ultimate reason there is a difference in M-M bonding while the M-L bonding is essentially the same on going from $Mo_2$ to $W_2$ is the presence of much larger cores (by 32 e) in the tungsten atoms. This has a negligible effect on the M-L bonds, but it causes the W-W bonds to be ca. 0.10 Å longer than the Mo-Mo bonds. The greater length considerably reduces the $\delta$ overlap, has a smaller but still significant adverse effect on the $\pi$ overlaps, and may also be responsible for reallocating d character among several orbitals with the symmetry appropriate for M-M $\sigma$ bonding.

**Acknowledgment.** We thank the National Science Foundation and the Department of Energy for financial support. Dr. Bruce E. Bursten and Mr. Jan Larsen carried out some preliminary calculations and Dr. B. W. S. Kolthammer prepared the samples used to record the PE spectra. D.L.L. is an Alfred P. Sloan Fellow, 1979-1981.

# $Na^+$ Complexes with Spiro-Bis-Crown Ethers: Stoichiometries, Stabilities, and Labilities in Pyridine Solution

**James Bouquant,[1] Alfred Delville, Jean Grandjean, and Pierre Laszlo***

*Contribution from the Institut de Chimie Organique et de Biochimie, Université de Liège, Sart-Tilman par 4000 Liège, Belgium.* *Received February 10, 1981*

**Abstract:** Complex formation between $NaClO_4$ and a series of crown ethers **1-4** has been studied by means of sodium-23 nuclear magnetic resonance, in pyridine solution. With the spiro-bis-crown ethers **2** and **3**, both 1:1 and 2:1 complexes are found to be present, corresponding to single and double occupation of the two equivalent binding sites offered by these dicoronands. With the monocrown ether **1**, as with the dicoronand **4** which presents an "$O_4$" ring interacting but weakly with $Na^+$, only 1:1 complexes form, in coexistence for **4** at high ligand ratios with 2:1 complexes. The 1:2 complexes are characterized by binding constants smaller by one order of magnitude, because of electrostatic repulsion between the two bound ions. Sodium ions appear to attach themselves to the first binding site at rates above $10^8$ $M^{-1}$ $s^{-1}$, close to diffusion control.

That crown ethers enjoy widespread use since their introduction[2] is almost an understatement. Therefore, it comes as no surprise that a number of studies have been directed at the precise determination of thermodynamic parameters[3] —and, also, of kinetic parameters[4] —for cation binding. Most of these studies[3,4] have relied upon ion-selective electrodes, calorimetry, or nuclear magnetic resonance methods. In an earlier article,[5] we have used multinuclear probes ($^1H$, $^{13}C$, and $^{23}Na$[6]) to investigate $Na^+$ complexation by linear polyethers. These mimic crown ethers by wrapping themselves around the alkali metal ion.[7] We report here on another structural variation, with respect to the main theme of crown ethers, when two such cyclic polyethers are linked together via a spiro junction.

One or two metallic ions will be able to attach themselves to such spiro bicycles (which have been named "dicoronands"). Presumably, the cavitites associated with the individual rings will be the sites of attachment. One would expect a decreased binding constant and a smaller association rate (or a larger dissociation rate) for interaction of the cation to the second ring, due to Coulombic repulsion with the occupant of the first site. One may also expect small conformation changes in the first ring, due to the presence of the second ring. In order to answer these and other questions, we have examined the organic ionophores listed in Scheme I. These ligands **1-4**, synthesized by Dr. E. Weber at the University of Bonn,[7] offer cavities of various sizes: from

(1) Laboratoire de chimie organique physique, UER Sciences, Université de Reims, BP 347, F-51962 Reims Cedex, France.

(2) Pedersen, C. J. *J. Am. Chem. Soc.* **1967**, *89*, 7017-7036. In "Synthetic Multidentate Macrocylic Compounds," Izatt, R. M., Christensen, J. J., Eds.; Academic Press: New York, 1978; pp 1-51.

(3) E.g.: Pedersen, C. J.; Frensdorff, H. K. *Angew. Chem., Int. Ed. Engl.* **1972**, *11*, 16-25. Frensdorff, H. K. *J. Am. Chem. Soc.* **1971**, *93*, 600-606. Lamb, J. D.; Izatt, R. M.; Swain, C. S.; Christensen, J. J. *Ibid.* **1980**, *102*, 475-479. Lamb, J. D.; Izatt, R. M.; Swain, C. S.; Bradshaw, J. S.; Christensen, J. J. *Ibid.* **1980**, *102*, 479-482.

(4) Shchori, E.; Jagur-Grodzinski, J.; Luz, Z.; Shporer, M. *J. Am. Chem. Soc.* **1971**, *93*, 7133-7138. Shchori, E.; Jagur-Grodzinski, J.; Shporer, M. *Ibid.* **1973**, *95*, 3842-3846. Degani, H. *Biophys. Chem.* **1977**, *6*, 345-349.

(5) Grandjean, J.; Laszlo, P.; Offermann, W.; Rinaldi, P. L. *J. Am. Chem. Soc.* **1981**, *103*, 1380-1383.

(6) Laszlo, P. *Angew. Chem., Int. Ed. Engl.* **1978**, *17*, 254-266; *Nachr. Chem., Tech. Lab.* **1979**, *27*, 710-712; *Bull. Magn. Reson*, in press.

(7) Vögtle, F.; Weber, E. *Angew. Chem., Int. Ed. Engl.* **1979**, *18*, 753-776. Weber, E.; Vögtle, F. *Inorg. Chim. Acta* **1980**, *45*, L65-L67.

0002-7863/82/1504-0686$01.25/0 